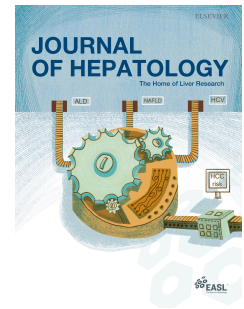


Journal Pre-proof

TGF- β -driven reduction of cytoglobin leads to oxidative DNA damage in stellate cells during non-alcoholic steatohepatitis

Yoshinori Okina, Misako Sato-Matsubara, Tsutomu Matsubara, Atsuko Daikoku, Lisa Longato, Krista Rombouts, Le Thi Thanh Thuy, Hiroshi Ichikawa, Yukiko Minamiyama, Mitsutaka Kadota, Hideki Fujii, Masaru Enomoto, Kazuo Ikeda, Katsutoshi Yoshizato, Massimo Pinzani, Norifumi Kawada



PII: S0168-8278(20)30228-2

DOI: <https://doi.org/10.1016/j.jhep.2020.03.051>

Reference: JHEPAT 7714

To appear in: *Journal of Hepatology*

Received Date: 27 August 2019

Revised Date: 28 March 2020

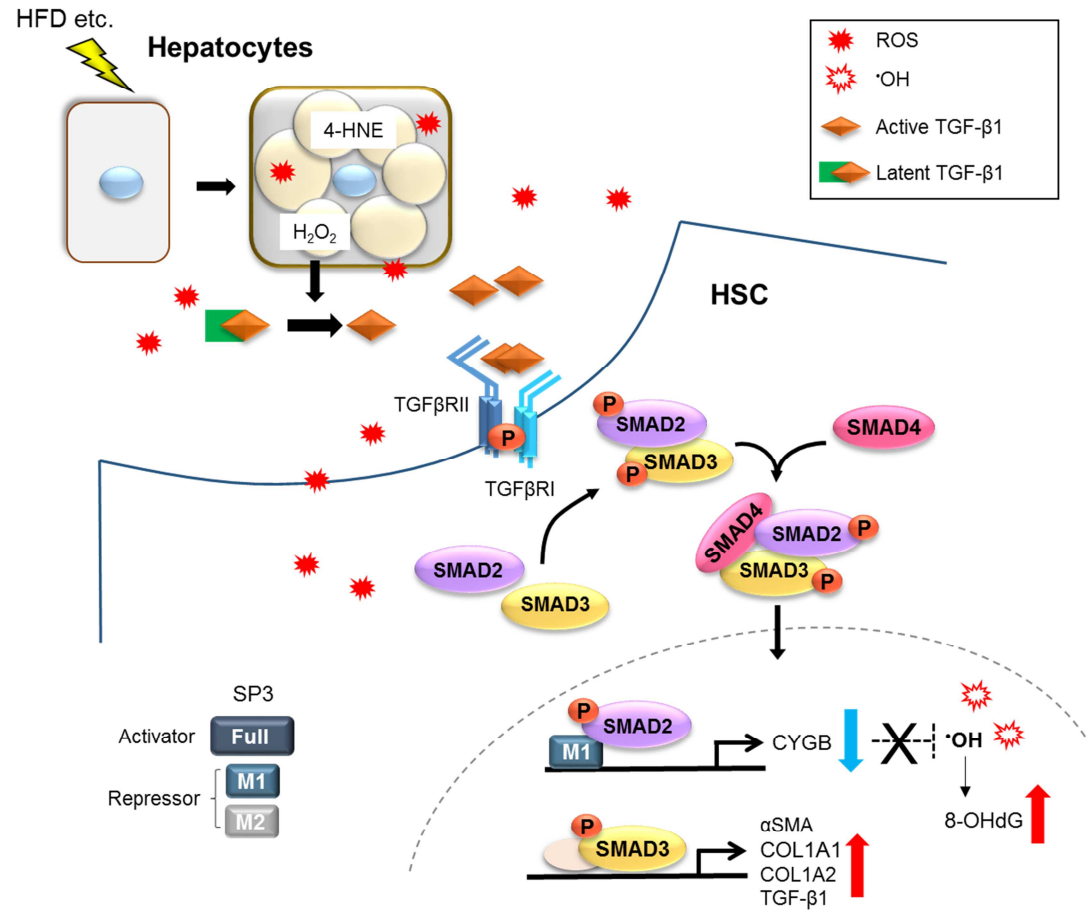
Accepted Date: 31 March 2020

Please cite this article as: Okina Y, Sato-Matsubara M, Matsubara T, Daikoku A, Longato L, Rombouts K, Thanh Thuy LT, Ichikawa H, Minamiyama Y, Kadota M, Fujii H, Enomoto M, Ikeda K, Yoshizato K, Pinzani M, Kawada N, TGF- β -driven reduction of cytoglobin leads to oxidative DNA damage in stellate cells during non-alcoholic steatohepatitis, *Journal of Hepatology* (2020), doi: <https://doi.org/10.1016/j.jhep.2020.03.051>.

This is a PDF file of an article that has undergone enhancements after acceptance, such as the addition of a cover page and metadata, and formatting for readability, but it is not yet the definitive version of record. This version will undergo additional copyediting, typesetting and review before it is published in its final form, but we are providing this version to give early visibility of the article. Please note that, during the production process, errors may be discovered which could affect the content, and all legal disclaimers that apply to the journal pertain.

© 2020 European Association for the Study of the Liver. Published by Elsevier B.V.

Graphical Abstract



TGF- β -driven reduction of cytoglobin leads to oxidative DNA damage in stellate cells during non-alcoholic steatohepatitis

Author Names: Yoshinori Okina^{1‡}, Misako Sato-Matsubara^{1,2‡}, Tsutomu Matsubara³, Atsuko Daikoku¹, Lisa Longato⁴, Krista Rombouts⁴, Le Thi Thanh Thuy¹, Hiroshi Ichikawa⁵, Yukiko Minamiyama⁶, Mitsutaka Kadota⁷, Hideki Fujii¹, Masaru Enomoto¹, Kazuo Ikeda³, Katsutoshi Yoshizato², Massimo Pinzani⁴, and Norifumi Kawada^{1*}

Author affiliation: Departments of Hepatology¹, Endowed Laboratory of Synthetic Biology², Anatomy and Regenerative Biology³, Graduate School of Medicine, Osaka City University, Osaka 545-8585, Japan; Regenerative Medicine and Fibrosis Group, Institute for Liver and Digestive Health, University College London, Royal Free Hospital, London, NW3 2PF, United Kingdom⁴; Department of Medical Life Systems, Faculty of Life and Medical Sciences, Doshisha University, Kyoto 610-0321, Japan⁵; and Food Hygiene and Environmental Health, Division of Applied Life Science, Graduate School of Life and Environmental Sciences, Kyoto Prefectural University, Kyoto 606-8522, Japan⁶, Laboratory for Phyloinformatics, RIKEN Center for Biosystems Dynamics Research, Hyogo 650-0047, Japan⁷

Note: ‡These authors contributed equally to this work.

***Corresponding author:** Norifumi Kawada, MD, PhD. Department of Hepatology, Graduate School of Medicine, Osaka City University, 1-4-3, Asahimachi, Abeno, Osaka 545-8585. Telephone: +81-6-6645-3897; Email: kawadanori@med.osaka-cu.ac.jp

Key words: NAFLD/NASH, liver fibrosis, cytoglobin, TGF- β 1, oxidative stress, hepatic stellate cells

Electronic word count: 6,984 words.

Number of figures and tables: 7 figures and 1 table. Supplementary information: 13 figures and 4 tables.

Conflicts of interest: All authors declare that they have no financial conflicts of interest to disclose.

Financial support statement: This work was supported by a Grant-in-Aid for Scientific Research (C) from JSPS KAKENHI 15K08314 (to MSM) and by a Grant-in-Aid for Scientific Research (B) from JSPS KAKENHI 16H05290 and a Grant

for Research Program on Hepatitis from the Japan Agency for Medical Research and Development (AMED – 18fk0210004h0003 and 19fk0210050h0001) (to NK).

Authors Contributions: YO, MSM, TM, and NK designed the experiments and interpreted the results. YO, MSM, AD and MK conducted the experiments. KR and LL provided and characterised the primary human HSCs. YO, MSM, TM, KR, LTTT, HI, YM, MK, HF, ME, KI, KY, MP, and NK wrote and revised the manuscript.

Abbreviations: α SMA, α -smooth muscle actin; ChIP, chromatin immunoprecipitation; COL1A1, collagen 1 α 1; COL1A2, collagen 1 α 2; CYGB, cytoglobin; ECM, extracellular matrix; ESR, electron spin resonance; FGF2, fibroblast growth factor 2; H₂O₂, hydrogen peroxide; HHStCs, human hepatic stellate cells; HSCs, hepatic stellate cells; 4-HNE, 4-hydroxy-2'-nonenal; IP, immunoprecipitation; MFBs, myofibroblasts; MTM, mithramycin A; NAFLD, non-alcoholic fatty liver disease; NAS, NAFLD Activity Score; NASH, NOX4, NADPH oxidase 4; non-alcoholic steatohepatitis; \cdot OH, hydroxyl radical; 8-OHdG, 8-hydroxy-2'-deoxyguanosine; Rh, recombinant human; ROS, reactive oxygen species; SteCM, stellate cell medium; TGF- β 1, transforming growth factor beta 1; TSS, transcription start site.

Abstract

Background and Aims: Cytoglobin (CYGB) is a respiratory protein that acts as a scavenger of reactive oxygen species. Although CYGB is expressed uniquely in hepatic stellate cells (HSCs) in the liver, the molecular role of CYGB in human HSC activation and human liver disease remains uncharacterised. The aim of this study was to reveal the mechanism by which TGF- β 1/SMAD2 pathway regulates human *CYGB* promoter and the pathophysiological function of CYGB in human non-alcoholic steatohepatitis (NASH).

Methods: Immunohistochemical staining was performed using human NASH biopsy specimens. Molecular and biochemical analysis were performed by western blotting, quantitative PCR, and luciferase and immunoprecipitation assays. Hydroxyl radicals (\cdot OH) and oxidative DNA damage were measured using an \cdot OH-detectable probe and 8-hydroxy-2'-deoxyguanosine (8-OHdG) ELISA.

Results: In culture, TGF- β 1-pretreated human hepatic stellate cells (HHStECs) exhibited lowered CYGB levels together with increased NADPH oxidase 4 (NOX4) expression and were primed for H₂O₂-triggered \cdot OH production and 8-OHdG generation. Overexpression of human CYGB in HHStECs cancelled out those effects of TGF- β 1. Electron spin resonance demonstrated direct \cdot OH-scavenging activity of recombinant

human *CYGB*. Mechanistically, pSMAD2 reduced *CYGB* transcription by recruiting the M1 repressor isoform of SP3 to the human *CYGB* promoter at nucleotide positions ^{+2–}⁺¹³ from the transcription start site. The same repression did not occur on the mouse *Cygb* promoter. TGF- β 1/SMAD3 mediated α SMA and collagen expression. Consistent with those observations in cultured HHStECs, *CYGB* expression was negligible, but 8-OHdG was abundant, in activated α SMA⁺pSMAD2⁺- and α SMA⁺NOX4⁺-positive hepatic stellate cells from human NASH patients with advanced fibrosis.

Conclusions: Downregulation of *CYGB* by the TGF- β 1/pSMAD2/SP3-M1 pathway brings about \cdot OH-dependent oxidative DNA damage in activated hepatic stellate cells from human patients with NASH.

Lay summary: TGF- β 1 downregulates human *CYGB* expression via SMAD2 phosphorylation and the M1 repressor isoform of SP3, giving rise to \cdot OH-induced 8-OHdG production in activated human hepatic stellate cells. Our findings provide new insights into the relationship between *CYGB* expression and the pathophysiology of NASH fibrosis in the human liver.

Introduction

Hepatic fibrosis is a common feature of many chronic liver diseases. Hepatic fibrosis ultimately progresses to cirrhosis and increases the risk of hepatocellular carcinoma (HCC) [1]. Severe hepatic fibrosis and HCC are estimated to cause 3.5% of all deaths worldwide [2], indicating a need for new anti-fibrotic therapies based on a detailed mechanistic understanding of liver disease [3]. The activation of hepatic stellate cells (HSCs) into contractile and matrix-producing myofibroblasts (MFBs) is a central event in liver fibrosis. HSC activation is triggered by multiple mediators secreted by damaged hepatocytes, activated macrophages, and aggregated platelets. Among the HSC-activating factors, transforming growth factor β 1 (TGF- β 1) is a key molecule that regulates MFB function [4]. In chronic liver disease, MFBs persist, become highly proliferative and migratory, and continuously deposit extracellular matrix (ECM) to replace hepatic parenchyma.

Cytoglobin (CYGB) is a mammalian globin expressed in HSCs that binds oxygen, carbon monoxide, and nitric oxide [5, 6] and protects organs and cells against oxidative stress [7, 8]. Recombinant rat Cygb was reported to increase the expression of antioxidant enzymes and to inhibit collagen (COL) III and IV expression in

CCl₄-induced liver fibrosis [9]. We previously demonstrated that *Cygb*^{-/-} mice are susceptible to diethylnitrosamine-induced development of liver cancer [10] and exhibit augmented hepatic inflammation, fibrosis, and tumour occurrence when fed a high-fat diet or subjected to bile-duct ligation [11, 12]. Conversely, thioacetamide-induced liver fibrosis was attenuated in HSC-specific *Cygb* transgenic mice [13].

The regulation of *CYGB* transcription and the role of *CYGB* in human fibrotic liver disease remain largely uncharacterised. *Cygb* expression was upregulated in mice exposed to hypoxia, whereas *Cygb* induction was lost in hypoxia-inducible factor 1 α -knockout mice [14]. Furthermore, hypoxia response elements were identified in the *Cygb* promoter region [15]. Those results suggest that the regulation of *Cygb* expression is oxygen dependent. By contrast, we recently reported that fibroblast growth factor 2 (FGF2) induces *CYGB* via c-JUN N-terminal kinase (JNK)-c-JUN signals in human HSCs [16].

Here, we show that TGF- β 1 suppresses human *CYGB* expression through phosphorylated SMAD2 (pSMAD2) and the M1 repressor isoform of SP3. The TGF- β 1-induced suppression of *CYGB* causes a loss of cellular tolerance to exogenous

oxidative stress and oxidative DNA damage in human HSCs. Our results provide a new insight into the pathophysiology of human NASH fibrosis.

Materials and Methods

Human tissue specimens. Patients with biopsy-proven non-alcoholic fatty liver disease (NAFLD)/non-alcoholic steatohepatitis (NASH) were recruited at Osaka City University Hospital (Osaka, Japan; Table 1). Thirteen liver biopsy specimens were obtained using a 16-gauge MAX-Core needle (Bard Biopsy Systems, AZ, USA). The samples were fixed in 10% formalin and stained with hematoxylin and eosin (H&E). Each specimen was evaluated by experienced pathologists that were blinded to the clinical findings.

ELISA for 8-OHdG. DNA was purified using a DNA Extract WB kit (Wako Pure Chemical Industries Ltd.) and subjected to ELISA for 8-OHdG according to the manufacturer's protocol. Intracellular 8-OHdG concentrations were measured by absorbance at 450 nm. The 8-OHdG standards used for the assay ranged between 0 ng/ml and 10 ng/ml.

Immunoprecipitation (IP) analysis. Cells were harvested with ice-cold PBS and lysed in TNE Buffer (50 mM Tris-HCl [pH 7.4], 0.1% NP-40, 100 mM NaCl, and 1 mM EDTA) containing protease inhibitors (Roche Diagnostics, Mannheim, Germany) and phosphatase inhibitors (Thermo Fisher Scientific, Waltham, MA, USA). The cell extracts (2 mg/450 μ l) were pre-cleaned with protein G magnetic beads (20 μ l of a 50%

bead slurry, Thermo Fisher Scientific) at 4°C for 60 min. The samples were then incubated with anti-SMAD2 antibody or normal rabbit IgG at 4°C overnight and subjected to SDS-PAGE by western blot analysis.

Statistics and reproducibility. All experiments were replicated at least three times.

Differences among experimental groups were analysed using unpaired *t*-test, Mann-Whitney U test, or one-way or two-way ANOVA performed using the GraphPad Prism 6 software (La Jolla, CA, USA). *P* values less than 0.05 were considered statistically significant. The data are displayed as the mean \pm standard deviation.

Significant differences among groups are indicated as **P* < 0.05, ***P* < 0.01, and ****P* < 0.001.

All information about the materials and methods are available in the Supplementary Information.

Results

Involvement of CYGB in reactive oxygen species (ROS) production and HSC activation in human liver fibrosis

Oxidative stress has been implicated in the pathogenesis of NAFLD/NASH with lobular inflammation and fibrosis [17]. We measured the expression of 4-hydroxy-2'-nonenal (4-HNE), an end product of lipid peroxidation, and 8-hydroxy-2'-deoxyguanosine (8-OHdG), a marker of oxidative DNA damage, in liver tissues from patients with biopsy-proven NAFLD/NASH with stage F0–F4 fibrosis (Table 1). As previously described [18], 4-HNE-positive staining was limited in patients with stage F0 fibrosis but was more pronounced in patients with more advanced fibrosis, especially those with stage F4 fibrosis ($P < 0.05$; **Fig. 1A**). A previous study reported that 4-HNE accumulated in destroyed hepatocytes and was discharged from those cells into the space of Disse [19], representing a source of oxidative stress in hepatic sinusoids. We did not observe any 8-OHdG-positive signal in cells from patients with stage F0 fibrosis, but 8-OHdG-staining was dominant in hepatocytes from patients with stage F1 fibrosis and abundant in both hepatocytes and stromal cells from patients with stage F4 fibrosis (**Fig. 1B** and Supplementary Fig. S1A). Double-immunohistochemical (IHC) staining revealed co-localisation of 8-OHdG and α -smooth muscle actin (α SMA) in the stroma

of patients with stage F4 disease (**Fig. 1C**).

Based on our observations of human NAFLD/NASH biopsy specimens, we hypothesised that activated HSCs become susceptible to oxidative stress. To confirm our hypothesis, we investigated the production of 2',7'-dichlorofluorescein diacetate (DCFDA)-detectable ROS in human HSC lines, HHSteCs and LX-2, which were pre-treated with rhTGF- β 1 and then stimulated with hydrogen peroxide (H_2O_2). Treatment with 2 ng/ml rhTGF- β 1 for 48 h resulted in slight increases in DCFDA-detectable ROS in the HHSteCs ($P < 0.05$). The combination of rhTGF- β 1 pre-treatment and subsequent H_2O_2 (0–640 μ M) treatment augmented the ROS production in a dose-dependent manner (**Fig. 1D**). Similar results were obtained in HHSteCs challenged with H_2O_2 in the presence of rhTGF- β 1, while LX-2, which lack CYGB expression, remained unresponsive to rhTGF- β 1 in H_2O_2 -dependent ROS production (Supplementary Fig. S2A and B). In addition, ROS production by these HSCs was reconfirmed by dihydroethidium (DHE) assay except for DCFDA assay (Supplementary Fig. S2C). To elucidate the reason why TGF- β 1 treatment enhanced ROS production in the HHSteCs, we analysed the expression of several genes associated with antioxidative cellular defence: *CYGB*, *SOD1*, *GSR*, *CAT*, *GPX1*, *GSS*,

PRDX1 and 2, *TXN* and *TXNRD1* in human HSCs. Of those genes, *CYGB* was the most strongly and dose-dependently downregulated by pre-treatment with rhTGF- β 1 in HHSteCs ($P < 0.00001$; **Fig. 1E** and Supplementary Fig. S3A). Likewise, these antioxidant genes were regulated by TGF- β 1 in LX-2, in which *CYGB* expression was lacking (Supplementary Fig. S3B). Furthermore, the overexpression of *CYGB* in HHSteCs and LX-2 transfected with pCMV6 vector containing human *CYGB* reduced the enhancement of DCFDA-detectable ROS production in response to 2 ng/ml rhTGF- β 1 followed by 320 μ M H₂O₂, returning the ROS levels to those observed after treatment with 320 μ M H₂O₂ alone (**Fig. 1F** and Supplementary Fig. S3C–D). Western blots of lysates of cells that were subjected to the same experimental conditions revealed that α SMA and COL1A were induced after the treatment with rhTGF- β 1 and/or H₂O₂, and that *CYGB* overexpression markedly reversed the induction at both protein and mRNA levels (**Fig. 1G** and Supplementary Fig. S4A). We also confirmed that TGF- β 1 significantly increased NADPH oxidase 4 (NOX4) and its expression was strongly reduced by the overexpression of *CYGB* (Supplementary Fig. S4A). These results indicated that *CYGB* is involved in the attenuation of HSC activation as well as the suppression of ROS production in human HSCs.

CYGB scavenges hydroxyl radical ($\cdot\text{OH}$) and protects TGF- β 1-activated HSCs from DNA damage

Because we observed accumulation of 8-OHdG in αSMA -positive stromal cells from patients with NASH with advanced fibrosis, we hypothesised that the suppression of CYGB expression by rhTGF- β 1 would result in the accumulation of oxidative DNA damage in HSCs due to $\cdot\text{OH}$, which is the causative agent of 8-OHdG formation [20]. To test that, we monitored mitochondrial ROS production using the mitochondria-specific probe MitoTracker[®] Red CM-H₂XRos. After pre-treatment for 48 h with 2 ng/ml rhTGF- β 1, HHSteCs were treated with 1 mM H₂O₂ for 1 h or with 100 μM antimycin A (ANT) or 100 μM pyocyanin (PYO) for 24 h to chemically induce $\cdot\text{OH}$ production. All three treatments induced MitoTracker[®] Red CM-H₂XRos-positive staining in HHSteCs pre-treated with rhTGF- β 1 (**Fig. 2A** and Supplementary Fig. S5A).

Next, we focused on mitochondrial $\cdot\text{OH}$ production using *in vivo* imaging analysis with OxiORANGE[™], a positively charged orange fluorescent probe that detects $\cdot\text{OH}$. We confirmed that pre-treatment with rhTGF- β 1 augmented cellular $\cdot\text{OH}$ accumulation in response to H₂O₂, ANT, or PYO treatment (**Fig. 2B** and Supplementary Fig. S5B). Conversely, overexpression of CYGB markedly suppressed the

rhTGF- β 1/H₂O₂-induced accumulation of \cdot OH in HHStECs (**Fig. 2C**). To evaluate the \cdot OH scavenging properties of CYGB, we performed electron spin resonance (ESR) spectroscopy using the CYPMPO spin trap. We observed dose-dependent decreases in the amplitude of the ESR signal with the addition of rhCYGB (0.025–0.2 mg/ml) (**Fig. 2D**). We converted the \cdot OH scavenging activity of 1 nmol rhCYGB to a 4.05 μ mol glutathione equivalent (**Fig. 2E**). The results revealed that mitochondrial \cdot OH levels were synergistically elevated by co-treatment with rhTGF- β 1 and H₂O₂ and that \cdot OH was scavenged by CYGB in HHStECs (**Fig. 2F**).

Next, we used 8-OHdG ELISA to measure cellular oxidative DNA damage in HHStECs after pre-treatment with 2 ng/ml rhTGF- β 1 for 48 h and subsequent exposure to 320 μ M H₂O₂ for 1 h. Treatment with rhTGF- β 1 alone did not affect 8-OHdG generation (0.56 ± 0.06 ng per 1 mg DNA). Treatment with H₂O₂ alone induced a comparatively small increase in 8-OHdG (1.04 ± 0.06 ng per 1 mg DNA). However, rhTGF- β 1 pre-treatment followed by H₂O₂ treatment induced cellular DNA damage at levels that were 3.6 times higher than those in untreated controls ($1.77 \text{ ng} \pm 0.03$ per 1 mg DNA; **Fig. 2G**). The overexpression of CYGB reduced the DNA damage levels, even after the combined treatment with rhTGF- β 1 and H₂O₂ (**Fig. 2H**). Thus, TGF- β 1 treatment followed by

H₂O₂ treatment, but not H₂O₂ treatment alone, triggered a reduction in CYGB, resulting in impaired scavenging defences against $\cdot\text{OH}$ and increased oxidative DNA damage in HHSteCs.

TGF- β 1 attenuates CYGB expression via SMAD2 and stimulates α SMA and Type I collagen expression via SMAD3

Next, we investigated the molecular regulatory mechanism of the TGF- β 1-induced downregulation of CYGB in HHSteCs. We used FGF2 as a CYGB inducer [16]. Treatment with 4 ng/ml FGF2 for 72 h increased CYGB expression and decreased α SMA expression at the protein and mRNA levels. By contrast, treatment with 2 ng/ml rhTGF- β 1 for 72 h downregulated CYGB expression and upregulated α SMA expression compared with that in untreated controls (**Fig. 3A** and Supplementary Fig. S6A). Other fibrosis-related growth factors (rhCTGF, PDGF-BB, and HGF) had negligible effects on CYGB protein expression (Supplementary Fig. S6B). Treatment with rhTGF- β 1 reduced CYGB and increased α SMA at both the protein level and the mRNA level in a dose-dependent (0–10 ng/ml) and time-dependent (0–48 h) manner (Supplementary Fig. S6C and D).

In HHSteCs, rhTGF- β 1 (2 ng/ml) phosphorylated canonical SMAD2 and SMAD3, starting at 15 min and reaching a peak at 1 h. In addition, ERK occurred at 1 h and 4 h, but it failed to activate the AKT and JNK pathways (**Fig. 3B** and Supplementary Fig. S6E–F). The TGF- β 1-dependent phosphorylation of SMAD2 and SMAD3 was completely blocked by 1 μ M SB431542 (Supplementary Fig. S7A). SB431542 also blocked the repression of CYGB expression as well as the induction of TGF- β 1-target genes such as α SMA, TGF- β 1, and COL1A1 in untreated and rhTGF- β 1-treated HHSteCs (**Fig. 3C** and **D**). To determine the specific SMAD involved in the TGF- β 1-induced repression of CYGB, we used shRNAs to stably inactivate SMAD2 or SMAD3 in HHSteCs. The shRNA sequences targeted to SMAD2 (shRNA Smad2) and SMAD3 (shRNA Smad3) resulted in 95.6% and 94.2% decreases in SMAD2 and SMAD3 protein levels, respectively (Supplementary Fig. S7B and C). ShRNA Smad2, but not shRNA GFP or shRNA Smad3, negated the TGF- β 1-induced downregulation of CYGB expression. Conversely, only shRNA Smad3 reduced the TGF- β 1-dependent induction of α SMA, COL1A1, and COL1A2 (**Fig. 3E** and **F**). Interestingly, depleting SMAD2 partially attenuated α SMA expression. Next, we confirmed treatment of 3 μ M SIS3 completely blocked the TGF- β 1-dependent phosphorylation of SMAD3, but not SMAD2 (Supplementary Fig. S7D). Furthermore, the treatment with SIS3 had no effect

on the rhTGF- β 1-induced CYGB expression, but it suppressed the induction of α SMA, COL1A1, and COL1A2 mRNAs (Supplementary Fig. S7E). To clarify whether SMAD4 is also part of the complex associated with the reduction of CYGB expression, we used siRNA strategy to knockdown SMAD4 in HHSteCs. SiSmad4 treatment inhibited the TGF- β 1-dependent induction of α SMA, COL1A1 and SERPINE1 and the reduction of CYGB (Supplementary Fig. S7F–H). Those results demonstrate that the TGF- β 1-SMAD2/SMAD4 pathway is involved in the reduction of CYGB expression, and the TGF- β 1-SMAD3/SMAD4 pathway is involved in the induction of α SMA, COL1A1, and COL1A2 in HHSteCs [21].

TGF- β 1 mediates the transcriptional repression of CYGB via an SP1/3 binding motif in the *CYGB* gene promoter in human HSCs, but not in mouse HSCs

TGF- β 1 reduced CYGB and increased α SMA and COL1A at the protein and mRNA levels in primary human HSCs isolated from the liver tissues of three patients (**Fig. 4A and B**). We also found that 0.4–10 ng/ml rhTGF- β 1 failed to repress Cygb expression but upregulated α Sma and Colla1 expression in primary cultured mouse HSCs (**Fig. 4C and D**). To determine the difference in CYGB gene regulation by rhTGF- β 1 between human and mouse HSCs, we investigated the transcriptional regulatory region of human

CYGB and mouse *Cygb* and found that an SP1/3 DNA binding motif was present at the transcription start site (TSS) in human *CYGB* but not in mouse *Cygb* (**Fig. 4E** and Supplementary Fig. S8A). SMAD2 has no DNA-binding ability and therefore requires the recruitment of transcriptional cofactors to transmit its regulatory signals [22]. To determine if the TGF- β 1/SMAD2-dependent suppression of *CYGB* expression is mediated by SP1/SP3, we used mithramycin A (MTM) to interrupt SP1/SP3 binding to the promoter region. Treatment of HHSteCs with 100 nM MTM completely blocked the TGF- β 1-dependent reduction in *CYGB* expression and the upregulation of α SMA, COL1A1, and COL1A2, which is reportedly mediated by the binding of SP1/SP3 protein in fibroblasts [23, 24] (**Fig. 4F and G**). Taken together, the results suggested that SP1 and/or SP3 is involved in the TGF- β 1-mediated downregulation of *CYGB* expression in HHSteCs.

The TGF- β 1/SMAD2 pathway specifically recruits the M1 repressor isoform of SP3 to the TSS and represses human *CYGB* promoter activity

To test our hypothesis that TGF- β 1/SMAD2 targets *CYGB* in human HSCs by recruiting SP1 and/or SP3 to the transcriptional regulatory region, we transfected HHSteCs with a human *CYGB* promoter construct containing the -2133 to +73 nucleotide sequence,

which includes the SP1/SP3 binding motif proximal to the TSS in exon 1 of *CYGB*. Treatment of the transfected cells with 2 ng/ml rhTGF- β 1 for 48 h resulted in a reduction of human *CYGB* promoter activity, but the reduction was completely abolished by treatment with 100 nM MTM (**Fig. 5A**). By contrast, rhTGF- β 1 did not reduce the promoter activity in HHSteCs transfected with a construct containing the -1726 to +114 nucleotide sequence of the mouse *Cygb* promoter (**Fig. 5B**). We also transfected primary mouse HSCs with the human *CYGB* or mouse *Cygb* promoter and measured the promoter activity to eliminate potential host effects. Our results indicated that rhTGF- β 1 reduced the activity of the human *CYGB* promoter but not that of the mouse *Cygb* promoter (**Fig. 5C**).

Next, to examine the binding of SP1 and/or SP3 to the human *CYGB* promoter, we constructed two mutated promoters (Mut-1 and Mut-2) with alterations at the SP1/3 DNA binding motif (5'-GTGGGCGGGCG-3'; labelled No. 4: $^{+2}-^{+13}$ nt in **Fig. 4E**). The inhibitory effect of rhTGF- β 1 on the *CYGB* promoter activity was abrogated in both mutants (**Fig. 5D**). Finally, to determine if SP1 or SP3 was involved in the repression of *CYGB* expression by rhTGF- β 1, we used SP1-specific and SP3-specific antibodies to conduct a chromatin immunoprecipitation (ChIP) assay of the *CYGB* promoter region

containing the SP1/3 binding motif in HHSteCs (**Fig. 5E**, left panel). Treatment with 2 ng/ml rhTGF- β 1 for 6 h amplified the *CYGB* promoter region that was pulled down by SP3-specific antibody, but not the region pulled down by SP1-specific antibody (**Fig. 5E**, right panel). The specificity of SP1-specific antibody was confirmed by amplifying the *COL1A2* promoter with the same ChIPped DNA (Supplementary Fig. S9A). Additionally, we confirmed the TGF- β 1-induced recruitment of SMAD2 to the same regulatory region of the *CYGB* promoter for SP3 binding (**Fig. 5F**). To evaluate the direct interaction between SMAD2 and SP3 in response to rhTGF- β 1, we conducted immunoprecipitation with a SMAD2-specific antibody in HHSteCs overexpressing SMAD2. On the basis of previous reports [25], we deduced that the protein band at 115 kDa corresponded to an activator (full) form of SP3 and that the lower bands were the M1 (70 kDa) and M2 (68 kDa) repressor forms of SP3 in whole-cell protein extracts (Input) (**Fig. 5G**, left panel). Our results demonstrated that, in parallel to the phosphorylation of SMAD2, which reached the highest level at 1 h after rhTGF- β 1 treatment (Supplementary Fig. S10A), the association of SMAD2 with SP3 isoform M1, but not that with full SP3 or isoform M2, was dramatically increased at 1 h and reduced at 4 h after rhTGF- β 1 treatment (**Fig. 5G**, right panel). Moreover, we confirmed a direct interaction between endogenous SMAD2 and SP3 isoform M1 in TGF- β 1-treated

HHSteCs (**Fig. 5H**). To evaluate whether the inhibitory complex between pSMAD2 and SP3 was induced transiently, the nuclear and cytoplasmic proteins isolated from HHSteCs were applied for immunoblot analysis, which confirmed the persistence of SMAD2 phosphorylation and its nuclear localisation up to 24 h after rhTGF- β 1 treatment (Supplementary Fig. S10B and C). Collectively, our results indicate that SMAD2 recruits the M1 repressor isoform of SP3 and suppresses *CYGB* promoter activity following rhTGF- β 1 treatment in HHSteCs.

CYGB expression in activated HSCs is negatively correlated with TGF- β 1/pSMAD2 signalling in human NASH with fibrosis

Following our observations in cultured human HSCs, we tested the relationship between *CYGB* expression and the activation of TGF- β 1/SMAD2 signalling in human NAFLD/NASH (Table 1). The different stages of fibrosis (F0, F1, and F4) of human NAFLD/NASH were demonstrated by H&E, Sirius Red, and IHC staining of *CYGB*, pSMAD2 and α SMA (**Fig. 6A** and Table 1). *CYGB*-positive HSCs were abundant in stages F0–2 but scarce in stages F3–4 ($P = 0.011$; **Fig. 6B**). Increased Sirius Red staining and IHC staining against pSMAD2 and α SMA was correlated with fibrosis progression ($P = 0.0016$; **Fig. 6A, 6C** and Supplementary Fig. S11A). These results

indicate that CYGB expression in human NASH is negatively correlated with fibrosis progression.

Absence of CYGB and pSMAD2 co-expression in activated HSCs along the septum of collagen fibres

In accordance with a previous report on hepatitis C virus-induced liver fibrosis [26], α SMA and pSMAD2 were co-localised in stromal cells, and the number of double-positive cells was greater in stage F3–4 fibrosis than in stage F0–2 fibrosis (**Fig. 7A**). IHC staining using NOX4 antibody showed the positivity of NOX4 in both hepatocytes and stromal cells, similar to pSMAD2 IHC staining. Furthermore, α SMA and NOX4 were also co-localised in stromal cells (Supplementary Fig. S12A and B). Furthermore, we observed CYGB-positive cells that were negative for pSMAD2 in liver stroma from patients with F1 fibrosis, whereas we detected no CYGB-positive cells proximal to pSMAD2-positive stromal cells in stroma from patients with F4 fibrosis (**Fig. 7B**). Finally, we observed the co-localisation of 8-OHdG and pSMAD2 in stroma from patients with stage F4 fibrosis (**Fig. 7C**). Taken together, the results indicate that TGF- β 1 signalling is strongly associated with the loss of CYGB and oxidative DNA damage in stromal cells in human NASH with advanced fibrosis.

Journal Pre-proof

Discussion

Our results revealed that the TGF- β 1/SMAD2/SP3-M1 signalling is a key pathway in the downregulation of human CYGB, which brings about the accumulation of intracellular \cdot OH and oxidative DNA damage in HSCs in human NASH with advanced fibrosis (**Fig. 7D**). Hepatic fibrosis can be defined as the persistent production and deposition of ECM by activated HSCs that are stimulated by gaseous, lipid, or peptide mediators secreted by damaged hepatocytes, mesenchymal cells, and inflammatory cells as a result of cell–cell interactions at the perivascular space [27]. Our results extend the understanding of the mode of TGF- β 1 action to encompass the downregulation of CYGB, which results in the exacerbation of oxidative DNA damage in human HSCs.

CYGB is highly conserved across species, with 84% and 99% homology between the human and mouse mRNA sequences and protein sequences, respectively (NCBI Blast, <https://blast.ncbi.nlm.nih.gov/Blast.cgi>). However, contrary to that in human livers with NASH (**Fig. 6A and B**), hepatic Cygb expression markedly increased in mice that were fed high-fat diet compared with that in mice that were fed a normal diet (Supplementary Fig. S13A). The difference in CYGB regulation between human and mouse livers meant

that we could not use *in vivo* mouse models of NASH to investigate the possible link between *Cygb* downregulation by TGF- β 1 and the accumulation of \cdot OH in HSCs. Instead, we investigated the mechanistic basis for the difference in transcriptional regulation of *CYGB* in response to TGF- β 1 between humans and mice. We identified an SP1/3 binding motif in the TSS of the human *CYGB* promoter that was absent in the mouse *Cygb* promoter. Previous reports showed that SP1/3 independently or cooperatively associates with SMAD2 or SMAD3 to induce COL1A1 and COL1A2 transcription and is also required for α SMA promoter activation in TGF- β 1-induced MFB differentiation [23, 24]. Furthermore, TGF- β induces the phosphorylation and nuclear translocation of SMAD2 and SMAD3 primarily in quiescent and activated HSCs, respectively, and these two SMADs have distinct roles in HSC activation [28]. In this study, we found that the TGF- β 1-mediated phosphorylation of SMAD2 in human HSCs triggered the recruitment of the M1 repressor isoform of SP3, but not that of other SP3 isoforms. A previous site-directed mutagenesis study revealed that SP1 binding to motifs at nucleotide positions -400, -230, and -210 of human *CYGB* resulted in the upregulation of *CYGB* expression; however, the SP1/3 binding motif at the TSS of our interest was not examined in that study [15]. Therefore, the position of the SP3 binding domain (+2) in the promoter region appears to be critical for *CYGB* downregulation.

Although the involvement of other transcriptional cofactors in the downregulation of CYGB by TGF- β 1 should be investigated, our results explain the discrepancy in CYGB gene expression between humans and mice.

In accordance with a previous report [29], we observed the accumulation of 4-HNE in hepatocytes of patients with NASH with advanced fibrosis. HSC activation in the injured liver is primarily initiated by ROS, products of lipid peroxidation, and TGF- β 1 released from destroyed/damaged hepatocytes, activated Kupffer cells, and infiltrating inflammatory cells [30, 31]. ROS and TGF- β 1 are also produced by HSCs in an autocrine manner in response to exogenous ROS and TGF- β 1 [32]. ROS convert latent TGF- β 1 to the active form [33], and activated TGF- β 1 promotes ROS formation by inducing NOX4, thereby creating a vicious cycle [34]. In this study, TGF- β 1-induced upregulation of NOX4 mRNA was suppressed by CYGB overexpression, suggesting that CYGB may directly regulate NOX4 expression. Furthermore, Fan *et al.* have recently reported that TGF- β 1 is secreted as a latent complex and deposited in the extracellular matrix of the healthy liver at a high concentration. They found that downregulation of extracellular matrix protein 1 in hepatocytes following liver injury strongly increased TGF- β signalling by spontaneously activating its extracellular

matrix-deposited latent form and consequently promoted HSC activation and fibrogenesis [35].

We investigated the expression levels of CYGB, GSR, PRDX2 and TXNRD1 in response to TGF- β 1 treatment and found that CYGB was the most significantly downregulated by TGF- β 1. In many cell types, the transcriptional response to oxidative stress is mediated by a cis-acting element termed the antioxidant response element (ARE); the nuclear factor E2-related factor 2 (Nrf2) has been identified as the most important transcription factor acting on the ARE for many antioxidant genes [36]. Our previous report showed increased Nrf2 expression and reduced TGF- β signalling in transgenic CYGB-overexpressing mouse HSCs [13]. These results suggest the possible coregulation of CYGB and other antioxidant genes by their upstream signalling.

The product of DNA oxidation, 8-OHdG, plays a significant role in mutagenesis because of its ability to pair with adenine and cytosine, causing genetic instability [37].

We observed increased 8-OHdG levels not only in hepatocytes [29] but also in MFBs in biopsy specimens from patients with NASH with advanced fibrosis. TGF- β enhanced the H₂O₂-induced accumulation of \cdot OH in HSCs following the downregulation of

CYGB expression (**Fig. 2B**). Furthermore, CYGB overexpression abrogated the excessive $\cdot\text{OH}$ generation in activated HSCs (**Fig. 2C**). Interestingly, our observation is supported by a recent study that has demonstrated the accumulation of somatic mutations in the cirrhotic liver, independent of carcinogenesis [38]. The TGF- β 1/SMAD2-induced DNA damage in HSCs in the NASH-fibrosis demonstrated in this study may be associated with early cancer development. Although further investigations of the relationship between oxidative DNA damage and HSC activation during fibrosis development are required, our data indicate that the impairment of antioxidative defence against aberrant $\cdot\text{OH}$ accumulation in HSCs is partly due to the downregulation of CYGB by TGF- β 1.

TGF- β 1/SMAD signalling has been shown to be central in the pathogenesis of liver fibrosis; therefore, targeting the TGF- β 1/SMAD pathway might be a useful therapeutic strategy for treating liver diseases [39]. At present, there are many strategies to block TGF- β 1 signalling. Treatment with neutralising TGF- β 1 antibodies or soluble human TGF- β receptor types I and II attenuated liver fibrosis in preclinical models [39, 40]. However, therapies targeting the TGF- β 1 pathway might also cause adverse outcomes due to pleiotropic effects. We previously reported that FGF2 acts as a CYGB inducer in

HSCs and promotes the downregulation of α SMA, COL1A1, COL1A2, and TGF- β 1. In addition, *in vivo* application of FGF2 attenuated the progression of liver fibrosis in a bile duct-ligation mouse model [16]. Furthermore, it was reported that overexpression of Cygb decreased urinary 8-OHdG excretion and ameliorated kidney fibrosis by suppressing oxidative damage in rats [41]. Thus, accumulating evidence suggests that CYGB plays both an anti-fibrotic role and a cyto-protective role, primarily through its antioxidative properties [10, 42], making it a candidate therapeutic molecule for liver disease.

In conclusion, human *CYGB* expression is downregulated by TGF- β 1 via a mechanism involving SMAD2 phosphorylation and the M1 repressor isoform of SP3. The downregulation of CYGB gives rise to \cdot OH-induced 8-OHdG production in activated human HSCs. Our findings provide new insights into the relationship between CYGB expression and the pathophysiology of NASH fibrosis in the human liver.

Acknowledgements

We would like to express our deepest appreciation to Dr. Lalage M. Wakefield (NCI, NIH), who provided us with the shRNA vectors and comments that greatly improved the manuscript. We also thank Mr. Yuta Noguchi (Doshisha University) for performing the ESR analysis, and the Osaka City University Graduate School of Medicine research support platform for technical assistance.

References

- [1] Fattovich G, Stroffolini T, Zagni I, Donato F. Hepatocellular carcinoma in cirrhosis: incidence and risk factors. *Gastroenterology* 2004;127:S35-50.
- [2] Asrani SK, Devarbhavi H, Eaton J, Kamath PS. Burden of liver diseases in the world. *Journal of hepatology* 2019;70:151-171.
- [3] Jun JI, Lau LF. Resolution of organ fibrosis. *The Journal of clinical investigation* 2018;128:97-107.
- [4] Weiskirchen R. Hepatoprotective and Anti-fibrotic Agents: It's Time to Take the Next Step. *Frontiers in pharmacology* 2015;6:303.
- [5] Sawai H, Kawada N, Yoshizato K, Nakajima H, Aono S, Shiro Y. Characterization of the heme environmental structure of cytoglobin, a fourth globin in humans. *Biochemistry* 2003;42:5133-5142.
- [6] Liu X, El-Mahdy MA, Boslett J, Varadharaj S, Hemann C, Abdelghany TM, et al. Cytoglobin regulates blood pressure and vascular tone through nitric oxide metabolism in the vascular wall. *Nature communications* 2017;8:14807.
- [7] Fordel E, Thijs L, Martinet W, Lenjou M, Laufs T, Van Bockstaele D, et al. Neuroglobin and cytoglobin overexpression protects human SH-SY5Y neuroblastoma cells against oxidative stress-induced cell death. *Neuroscience letters*

2006;410:146-151.

[8] Hodges NJ, Innocent N, Dhanda S, Graham M. Cellular protection from oxidative DNA damage by over-expression of the novel globin cytoglobin in vitro. *Mutagenesis* 2008;23:293-298.

[9] Li Z, Wei W, Chen B, Cai G, Li X, Wang P, et al. The Effect of rhCygb on CCl4-Induced Hepatic Fibrogenesis in Rat. *Scientific reports* 2016;6:23508.

[10] Thuy le TT, Matsumoto Y, Thuy TT, Hai H, Suoh M, Urahara Y, et al. Cytoglobin deficiency promotes liver cancer development from hepatosteatosi through activation of the oxidative stress pathway. *The American journal of pathology* 2015;185:1045-1060.

[11] Thuy le TT, Morita T, Yoshida K, Wakasa K, Iizuka M, Ogawa T, et al. Promotion of liver and lung tumorigenesis in DEN-treated cytoglobin-deficient mice. *The American journal of pathology* 2011;179:1050-1060.

[12] Van Thuy TT, Thuy LT, Yoshizato K, Kawada N. Possible Involvement of Nitric Oxide in Enhanced Liver Injury and Fibrogenesis during Cholestasis in Cytoglobin-deficient Mice. *Scientific reports* 2017;7:41888.

[13] Thi Thanh Hai N, Thuy LTT, Shiota A, Kadono C, Daikoku A, Hoang DV, et al. Selective overexpression of cytoglobin in stellate cells attenuates thioacetamide-induced

liver fibrosis in mice. *Scientific reports* 2018;8:17860.

[14] Fordel E, Geuens E, Dewilde S, De Coen W, Moens L. Hypoxia/ischemia and the regulation of neuroglobin and cytoglobin expression. *IUBMB life* 2004;56:681-687.

[15] Guo X, Philipsen S, Tan-Un KC. Characterization of human cytoglobin gene promoter region. *Biochimica et biophysica acta* 2006;1759:208-215.

[16] Sato-Matsubara M, Matsubara T, Daikoku A, Okina Y, Longato L, Rombouts K, et al. Fibroblast growth factor 2 (FGF2) regulates cytoglobin expression and activation of human hepatic stellate cells via JNK signaling. *The Journal of biological chemistry* 2017;292:18961-18972.

[17] Duvnjak M, Lerotic I, Barsic N, Tomasic V, Virovic Jukic L, Velagic V. Pathogenesis and management issues for non-alcoholic fatty liver disease. *World journal of gastroenterology* 2007;13:4539-4550.

[18] Paradis V, Mathurin P, Kollinger M, Imbert-Bismut F, Charlotte F, Piton A, et al. In situ detection of lipid peroxidation in chronic hepatitis C: correlation with pathological features. *Journal of clinical pathology* 1997;50:401-406.

[19] Gandhi CR. Oxidative Stress and Hepatic Stellate Cells: A PARADOXICAL RELATIONSHIP. *Trends in cell & molecular biology* 2012;7:1-10.

[20] Arimoto T, Yoshikawa T, Takano H, Kohno M. Generation of reactive oxygen

species and 8-hydroxy-2'-deoxyguanosine formation from diesel exhaust particle components in L1210 cells. Japanese journal of pharmacology 1999;80:49-54.

[21] Uemura M, Swenson ES, Gaca MD, Giordano FJ, Reiss M, Wells RG. Smad2 and Smad3 play different roles in rat hepatic stellate cell function and alpha-smooth muscle actin organization. Molecular biology of the cell 2005;16:4214-4224.

[22] Zawel L, Dai JL, Buckhaults P, Zhou S, Kinzler KW, Vogelstein B, et al. Human Smad3 and Smad4 are sequence-specific transcription activators. Molecular cell 1998;1:611-617.

[23] Cogan JG, Subramanian SV, Polikandriotis JA, Kelm RJ, Jr., Strauch AR. Vascular smooth muscle alpha-actin gene transcription during myofibroblast differentiation requires Sp1/3 protein binding proximal to the MCAT enhancer. The Journal of biological chemistry 2002;277:36433-36442.

[24] Zhang W, Ou J, Inagaki Y, Greenwel P, Ramirez F. Synergistic cooperation between Sp1 and Smad3/Smad4 mediates transforming growth factor beta1 stimulation of alpha 2(I)-collagen (COL1A2) transcription. The Journal of biological chemistry 2000;275:39237-39245.

[25] Ammanamanchi S, Brattain MG. Sp3 is a transcriptional repressor of transforming growth factor-beta receptors. The Journal of biological chemistry

2001;276:3348-3352.

[26] Motoyama H, Komiya T, Thuy le TT, Tamori A, Enomoto M, Morikawa H, et al. Cytoglobin is expressed in hepatic stellate cells, but not in myofibroblasts, in normal and fibrotic human liver. *Laboratory investigation; a journal of technical methods and pathology* 2014;94:192-207.

[27] Friedman SL. Mechanisms of disease: Mechanisms of hepatic fibrosis and therapeutic implications. *Nature clinical practice Gastroenterology & hepatology* 2004;1:98-105.

[28] Liu C, Gaca MD, Swenson ES, Vellucci VF, Reiss M, Wells RG. Smads 2 and 3 are differentially activated by transforming growth factor-beta (TGF-beta) in quiescent and activated hepatic stellate cells. Constitutive nuclear localization of Smads in activated cells is TGF-beta-independent. *The Journal of biological chemistry* 2003;278:11721-11728.

[29] Seki S, Kitada T, Yamada T, Sakaguchi H, Nakatani K, Wakasa K. In situ detection of lipid peroxidation and oxidative DNA damage in non-alcoholic fatty liver diseases. *Journal of hepatology* 2002;37:56-62.

[30] Lee KS, Buck M, Houghlum K, Chojkier M. Activation of hepatic stellate cells by TGF alpha and collagen type I is mediated by oxidative stress through c-myb

expression. The Journal of clinical investigation 1995;96:2461-2468.

[31] Parola M, Pinzani M, Casini A, Albano E, Poli G, Gentilini A, et al. Stimulation of lipid peroxidation or 4-hydroxynonenal treatment increases procollagen alpha 1 (I) gene expression in human liver fat-storing cells. Biochemical and biophysical research communications 1993;194:1044-1050.

[32] De Bleser PJ, Xu G, Rombouts K, Rogiers V, Geerts A. Glutathione levels discriminate between oxidative stress and transforming growth factor-beta signaling in activated rat hepatic stellate cells. The Journal of biological chemistry 1999;274:33881-33887.

[33] Wang H, Kochevar IE. Involvement of UVB-induced reactive oxygen species in TGF-beta biosynthesis and activation in keratinocytes. Free radical biology & medicine 2005;38:890-897.

[34] Proell V, Carmona-Cuenca I, Murillo MM, Huber H, Fabregat I, Mikulits W. TGF-beta dependent regulation of oxygen radicals during transdifferentiation of activated hepatic stellate cells to myofibroblastoid cells. Comparative hepatology 2007;6:1.

[35] Fan W, Liu T, Chen W, Hammad S, Longerich T, Hausser I, et al. ECM1 Prevents Activation of Transforming Growth Factor beta, Hepatic Stellate Cells, and

Fibrogenesis in Mice. *Gastroenterology* 2019;157:1352-1367 e1313.

[36] Nguyen T, Nioi P, Pickett CB. The Nrf2-antioxidant response element signaling pathway and its activation by oxidative stress. *The Journal of biological chemistry* 2009;284:13291-13295.

[37] Maki H, Sekiguchi M. MutT protein specifically hydrolyses a potent mutagenic substrate for DNA synthesis. *Nature* 1992;355:273-275.

[38] Zhu M, Lu T, Jia Y, Luo X, Gopal P, Li L, et al. Somatic Mutations Increase Hepatic Clonal Fitness and Regeneration in Chronic Liver Disease. *Cell* 2019;177:608-621 e612.

[39] Xu F, Liu C, Zhou D, Zhang L. TGF-beta/SMAD Pathway and Its Regulation in Hepatic Fibrosis. *The journal of histochemistry and cytochemistry : official journal of the Histochemistry Society* 2016;64:157-167.

[40] Akhurst RJ. Targeting TGF-beta Signaling for Therapeutic Gain. *Cold Spring Harbor perspectives in biology* 2017;9.

[41] Mimura I, Nangaku M, Nishi H, Inagi R, Tanaka T, Fujita T. Cytooglobin, a novel globin, plays an antifibrotic role in the kidney. *American journal of physiology Renal physiology* 2010;299:F1120-1133.

[42] Li D, Chen XQ, Li WJ, Yang YH, Wang JZ, Yu AC. Cytooglobin up-regulated

by hydrogen peroxide plays a protective role in oxidative stress. *Neurochemical research* 2007;32:1375-1380.

Table 1.

Characteristics	all (n = 13)	No Advanced Fibrosis (stage 0-2) (n = 8)	Advanced Fibrosis (stage 3-4) (n = 5)	p-value*
Demographics				
Age (years)	55.9 ± 15.1	51.1 ± 17.7	63.6 ± 3.7	0.377
Gender				0.075
Female	8 (61.5)	3 (37.5)	5 (100.0)	
Male	5 (38.5)	5 (62.5)	0 (0.0)	
BMI (kg/m ²)	26.3 ± 3.3	26.5 ± 3.5	26.1 ± 3.4	0.770
Biological Data				
AST (U/L)	50.2 ± 29.9	47.5 ± 33.8	54.6 ± 25.2	0.341
ALT (U/L)	63.8 ± 52.4	70.5 ± 61.5	53.2 ± 37.3	0.942
GGT (U/L)	75.1 ± 42.8	84.4 ± 49.6	60.2 ± 27.0	0.341
Total Bilirubin (mg/dL)	0.86 ± 0.24	0.80 ± 0.26	0.96 ± 0.19	0.262
Direct Bilirubin (mg/dL)	0.29 ± 0.08	0.29 ± 0.08	0.3 ± 0.07	0.753
Albumin (g/dL)	4.1 ± 0.38	4.3 ± 0.27	3.8 ± 0.34	0.022
Triglycerides (mg/dL)	99.2 ± 35.3	104.6 ± 37.6	90.4 ± 33.2	0.770
Total Cholesterol (mg/dL)	187.6 ± 40.9	184.8 ± 36.0	192.2 ± 51.9	0.999
Platelet Count (10 ⁹ /L)	207.8 ± 68.9	239.4 ± 49.7	157.2 ± 68.7	0.040
Glucose (mg/dL)	120.8 ± 34.9	131.9 ± 40.0	103.0 ± 14.1	0.164
Clinical Prediction Rules				
NAFLD Fibrosis Score	0.09 ± 0.93	0.07 ± 0.62	0.11 ± 1.38	0.884
FIB-4 index	2.15 ± 1.42	1.34 ± 0.89	3.43 ± 1.14	0.008
Histology				
NAS n (%)				
Steatosis				
0	1 (7.7)	1 (12.5)	0 (0.0)	
1	6 (46.2)	3 (37.5)	3 (60.0)	
2	3 (23.1)	1 (12.5)	2 (40.0)	
3	3 (23.1)	3 (37.5)	0 (0.0)	
Ballooning				
0	6 (46.2)	6 (75.0)	0 (0.0)	
1	2 (15.4)	0 (0.0)	2 (40.0)	
2	5 (38.5)	2 (25.0)	3 (60.0)	
Inflammation				
0	3 (23.1)	3 (37.5)	0 (0.0)	
1	5 (38.5)	4 (50.0)	1 (20.0)	
2	3 (23.1)	0 (0.0)	3 (60.0)	
3	2 (15.4)	1 (12.5)	1 (20.0)	
Fibrosis n (%)				
0	2 (15.4)	2 (25.0)	0 (0.0)	
1	4 (30.8)	4 (50.0)	0 (0.0)	
2	2 (15.4)	2 (25.0)	0 (0.0)	
3	3 (23.1)	0 (0.0)	3 (60.0)	
4	2 (15.4)	0 (0.0)	2 (40.0)	

Table 1. Clinical and biochemical characteristics of the patients with biopsy-proven NAFLD/NASH.

Abbreviations: ALT, alanine aminotransferase; AST, aspartate aminotransferase; BMI, body mass index; FIB-4, fibrosis-4; GGT, γ -glutamyltranspeptidase; NAFLD, non-alcoholic fatty liver disease; NAS, NAFLD Activity Score; NASH, non-alcoholic steatohepatitis. *P*-values were obtained using *t*-test for continuous variables.

Figure Legends

Fig. 1. Relationship between CYGB repression and intracellular ROS accumulation in activated HSCs and human liver tissues. (A and B) NAFLD/NASH specimens stained with (A) 4-HNE and (B) 8-OHdG (brown). Positive areas in (A) compared by *t*-test, $n = 13$ (F0 $n = 2$, F1 $n = 4$, F4 $n = 2$). **(C)** Double-positive (8-OHdG/ α SMA) stage-F4 stromal cells. Bars, 5 μ m. **(D)** Intracellular ROS production. RFU: relative fluorescence unit. Relative fold change of DCFDA-detectable ROS production in response to 2 ng/ml rhTGF- β 1 followed by H₂O₂ (0–640 μ M) treatment compared with that in untreated controls. **(E)** Relative mRNA expression. #, difference by multiple *t*-tests with FDR of 1%. **(F)** Intracellular ROS production in cells transfected with pCMV6 empty vector (EV) or pCMV6-(CYGB). **(G)** Protein expression in transfected cells. Data expressed as means \pm SD, $n = 3$. * $P < 0.05$, ** $P < 0.01$, and *** $P < 0.001$ by ANOVA. Bars, 25 μ m or 100 μ m (enlarged views).

Fig. 2. The role of CYGB in $\cdot\text{OH}$ accumulation and cellular DNA damage induced by TGF- β 1 and H_2O_2 in human HSCs. (A and B) H_2O_2 -induced mitochondrial ROS (red, A) and intracellular $\cdot\text{OH}$ (orange, B) after TGF- β 1 treatment. **(C)** Effect of CYGB overexpression on intracellular $\cdot\text{OH}$ generation. EV: pCMV6 empty vector. Immunofluorescence for human CYGB (green, upper) and OxiORANGETM (orange, lower). **(D)** Scavenging of $\cdot\text{OH}$ by rhCYGB determined by ESR. MnO: manganese (II) oxide; mT: milliTesla; §: peak amplitude. **(E)** Concentration of rhCYGB converted to glutathione equivalent. **(F)** Formation of $\cdot\text{OH}$ and action of antioxidative genes. **(G)** Intracellular 8-OHdG formation in HHStECs. **(H)** Effect of CYGB overexpression on 8-OHdG formation (ng) per 1 mg DNA. Data expressed as means \pm SD, $n = 3$. ns: not significant; *** $P < 0.001$ by ANOVA. Bars, 20 μm .

Fig. 3. Effect of TGF- β 1 on CYGB and α SMA expression. (A) Effect of rhFGF2 or rhTGF- β 1 on CYGB and α SMA expression in HHSteCs. (B) Expression of total and phosphorylated SMAD2 and SMAD3. (C) Effect of SB431542 on relative CYGB and α SMA protein expression. (D) Effect of SB431542 on relative mRNA expression. (E) Relative CYGB and α SMA protein expression in HHSteCs transfected with shSmad2 or shSmad3. Bar graphs show relative intensities normalised to GAPDH compared with untreated controls (A, C and E). (F) mRNA levels in HHSteCs transfected with shRNAs. Data expressed as means \pm SD, $n = 3$. ns: not significant; * $P < 0.05$, ** $P < 0.01$, and *** $P < 0.001$ by ANOVA.

Fig. 4. The effect of TGF- β 1 on CYGB expression in human and mouse HSCs. (A, B) Effect of TGF- β 1 on protein and mRNA levels in human HSCs assayed by western blot (A) and qRT-PCR (B). **(C and D)** Protein and mRNA levels in mouse HSCs assayed by western blot (C) and qRT-PCR (D). **(E)** Putative SP1/3 binding motifs (grey bar). Striped grey bar indicates the motif of interest (No. 4). Transcription start site: TSS. **(F)** Effect of MTM on relative protein expression in HHSteCs treated with rhTGF- β 1 (two-way ANOVA-Dunnett's). **(G)** Effect of MTM on relative mRNA expression. Data expressed as means \pm SD, $n = 3$. ns: not significant; * $P < 0.05$, ** $P < 0.01$, and *** $P < 0.001$ two-tailed unpaired t -test (B and D) or ANOVA (G).

Fig. 5. Regulation of CYGB expression by the M1 repressor isoform of SP3 in TGF- β 1-treated HHSteCs. (A) *CYGB* promoter activity in (*CYGB*)-transfected HHSteCs. (B) *Cygb* promoter activity in (*Cygb*)-transfected HHSteCs. (C) *CYGB* promoter activity in mouse HSCs. (D) Luciferase reporter fused to wild-type (WT) and mutated human *CYGB* promoters (underlined). The pGL4.10-EV vector was used as a control. RLU: relative light unit. (E) ChIP using antibodies against SP1 and SP3 and primers targeting the SP1/3-binding motif (grey bar with oblique line). Results analysed by semi-qPCR and presented as fold enrichment relative to total input DNA. IgG was used as a control. (F) ChIP assay of SMAD2 at human *CYGB* promoter was analysed by quantitative RT-PCR. *** $P < 0.001$ by unpaired t -test compared with untreated control. (G) IP for the SMAD2-binding protein with TGF- β 1 treatment at indicated time points. (H) IP for endogenous SMAD2-binding protein. Data expressed as means \pm SD, $n = 3$. ns: not significant; *** $P < 0.001$ by ANOVA (A–D) or two-tailed unpaired t -test (E).

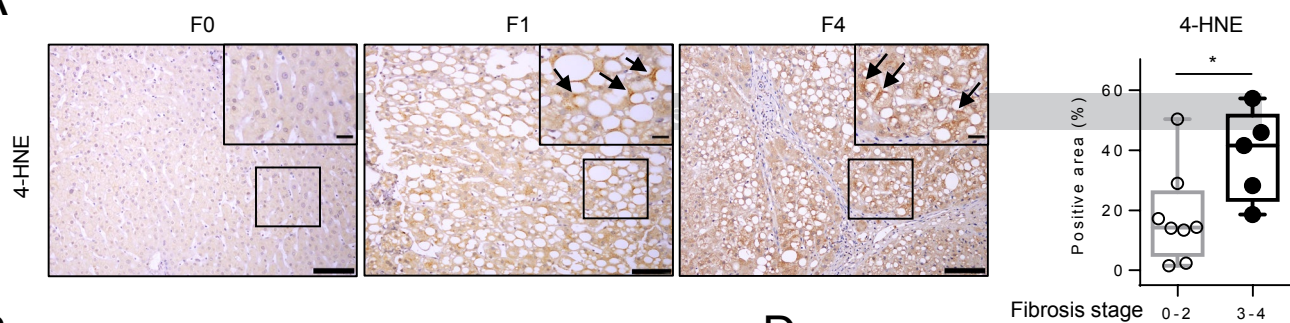
Fig. 6. Expression of CYGB, pSMAD2, and α SMA in human NAFLD/NASH biopsy specimens. (A) NAFLD/NASH specimens with the indicated staining. Total $n = 13$; fibrosis stage F0 ($n = 2$), stage F1 ($n = 4$), and stage F4 ($n = 2$). Arrows, positive cells. Magnified images indicate the same area in each of the stained samples. Bars, 50 μm . (B) Quantification of CYGB-positive cells per 1 mm^2 of biopsy specimen. (C) Quantification of Sirius Red-positive and α SMA-positive areas. Data expressed as means \pm SD, $n = 13$ (F0–2, $n = 8$; F3–4, $n = 5$). $**P < 0.01$, two-tailed unpaired t -test (B and C) (see Table 1).

Fig. 7. The association between CYGB and pSMAD2 expression in stromal cells from patients with liver fibrosis. (A) Biopsy of fibrosis stage F0 ($n = 2$) or F4 ($n = 2$) stained with α SMA (green) or pSMAD2 (red). Arrows, pSMAD2⁺ α SMA⁺ cells. Bars, 20 μ m. Quantification of pSMAD2⁺ α SMA⁺ cells. Data expressed as means \pm SD; total $n = 13$. ** $P < 0.01$; two-tailed unpaired t -test. (B) Biopsies of F1 fibrosis or F4 fibrosis stained with CYGB (green) and pSMAD2 (red). Arrows, CYGB⁺pSMAD2⁻ stromal cells. Bars, 50 μ m. (C) Immunofluorescence of 8-OHdG (green) and pSMAD2 (red) in F4 fibrosis. Arrows, 8-OHdG⁺pSMAD2⁺ stromal cells. DAPI was used for nuclear staining. Bars, 20 μ m. (D) CYGB involvement in TGF- β 1-induced human HSC activation and liver fibrosis. HFD, high-fat diet; HSC, hepatic stellate cell.

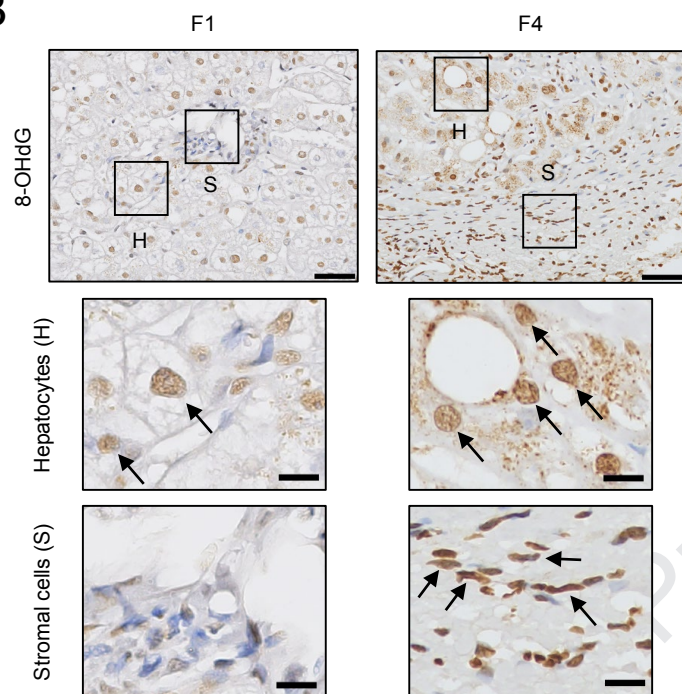
Highlights

- Reactive oxygen species levels are increased in advanced human NASH fibrosis.
- CYGB directly scavenges $\cdot\text{OH}$ and attenuates 8-OHdG generation in human HSCs.
- CYGB downregulation by TGF- β 1 leads to oxidative DNA damage in human HSCs.
- TGF- β 1 suppresses *CYGB* expression in human HSCs via the pSMAD2/SP3-M1 pathway.
- CYGB expression is absent in pSMAD2⁺8-OHdG⁺ HSCs in human NASH fibrosis.

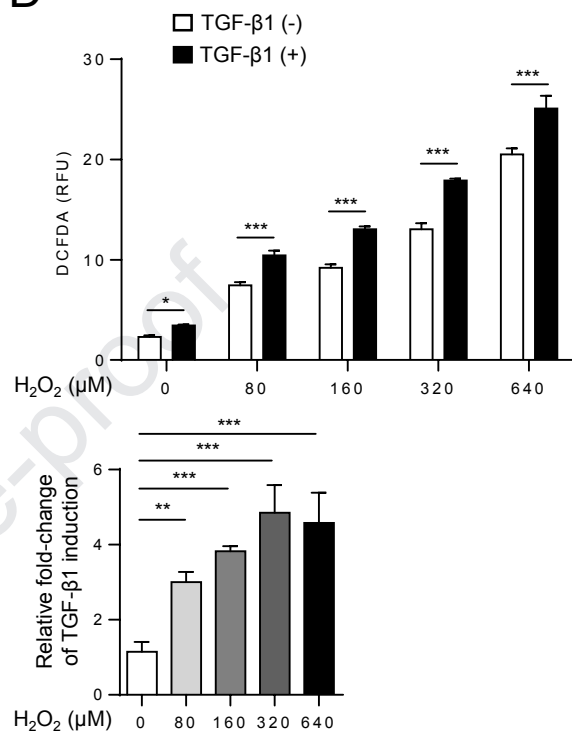
A



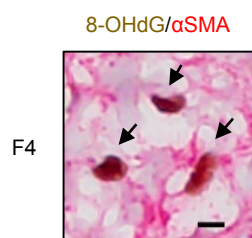
B



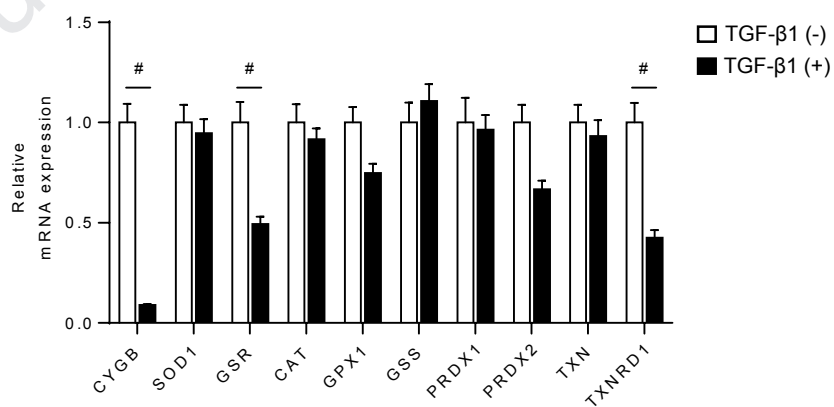
D



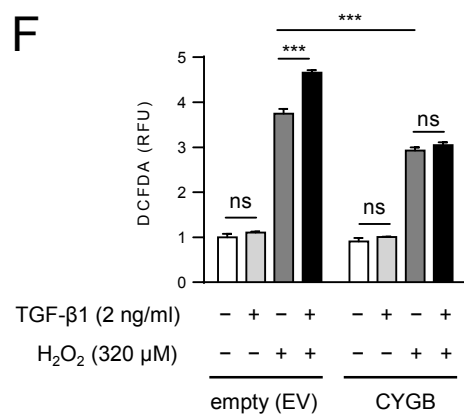
C



E



F



G

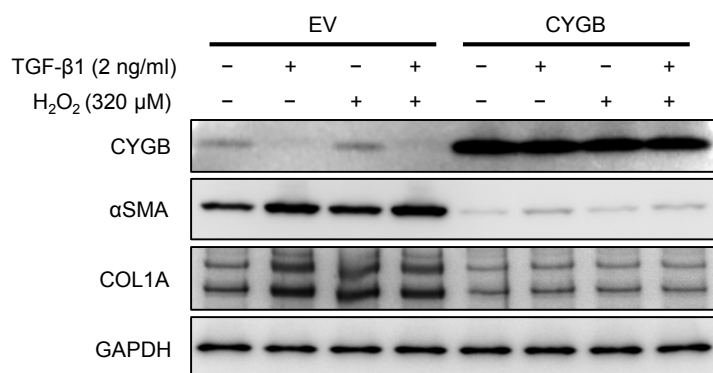


Figure 1

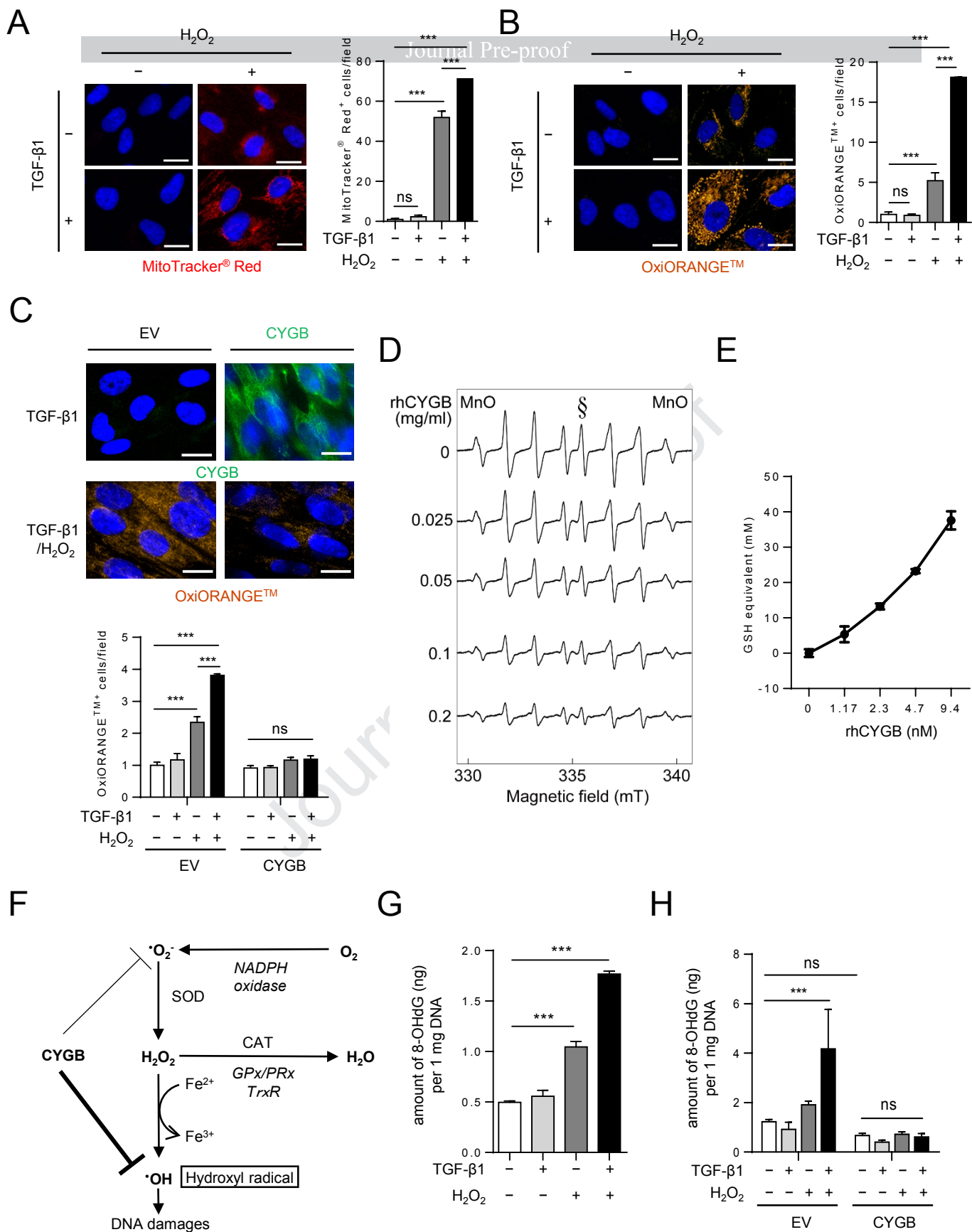
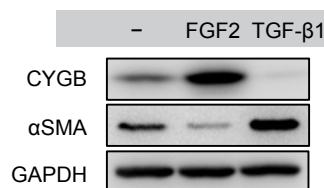
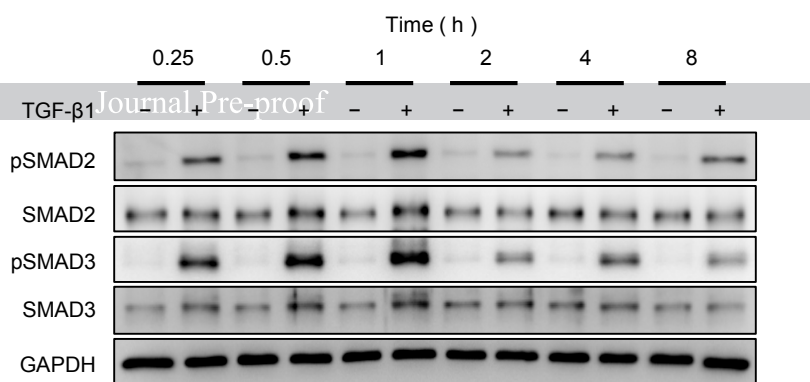


Figure 2

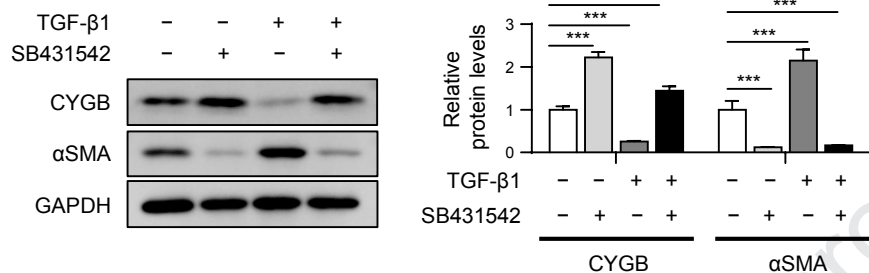
A



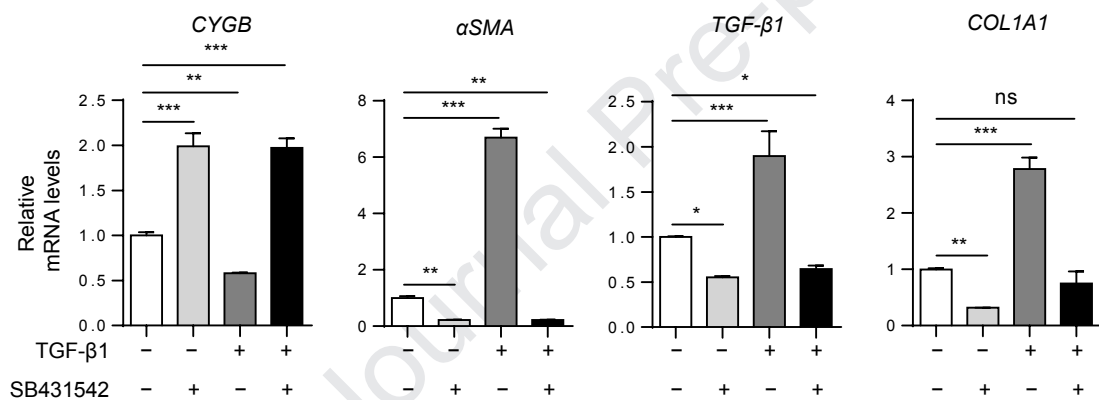
B



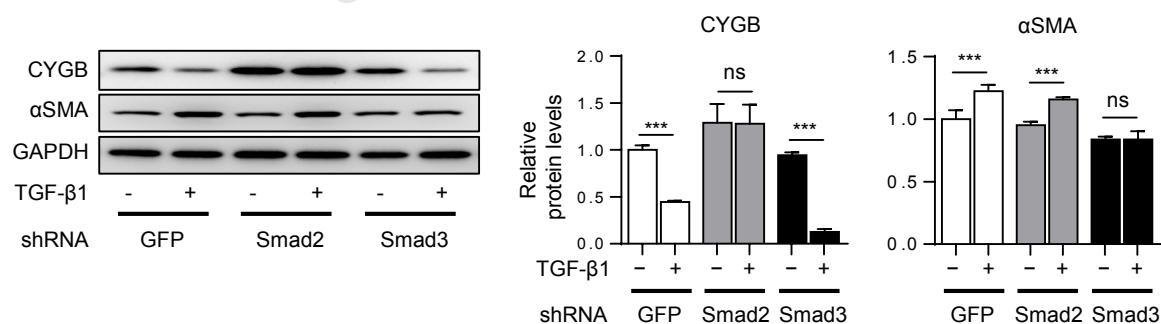
C



D



E



F

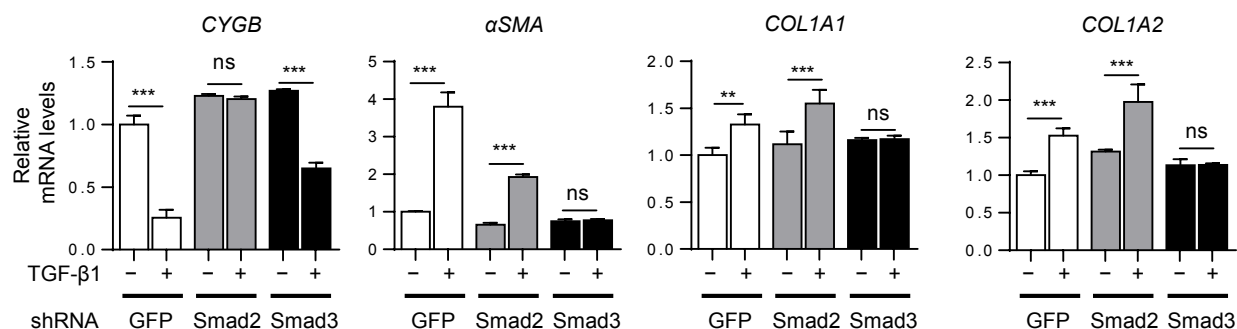
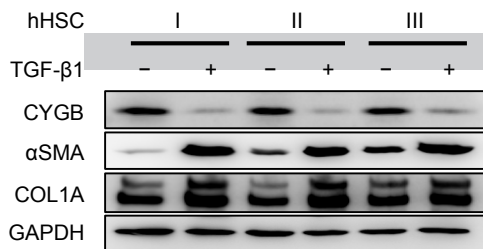
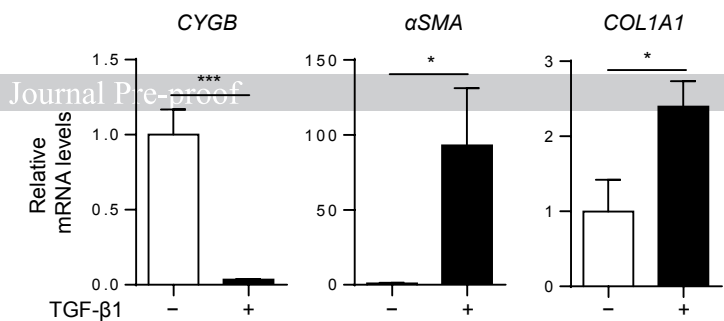


Figure 3

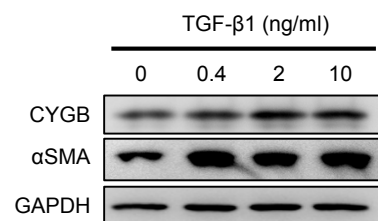
A



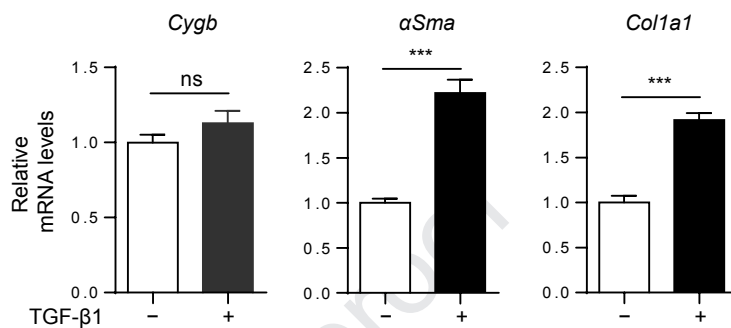
B



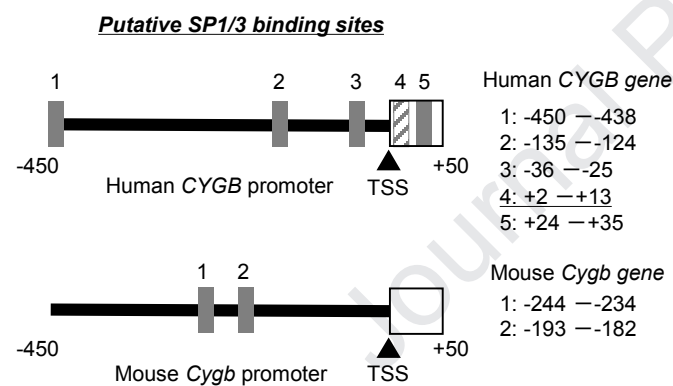
C



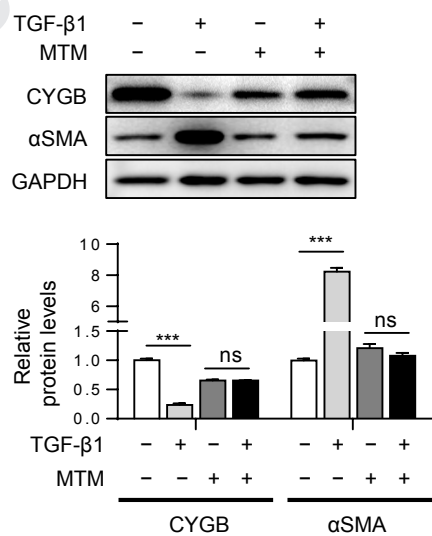
D



E



F



G

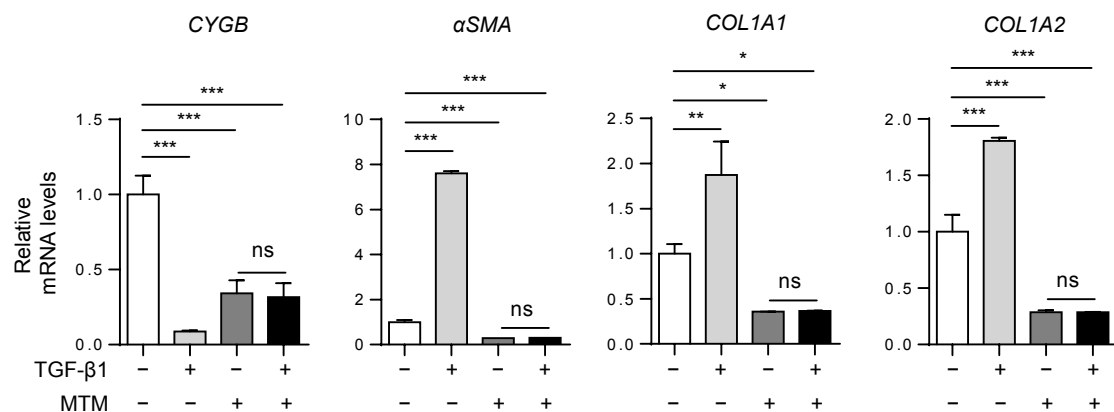
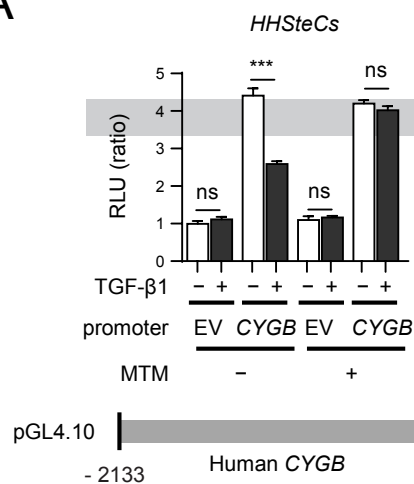
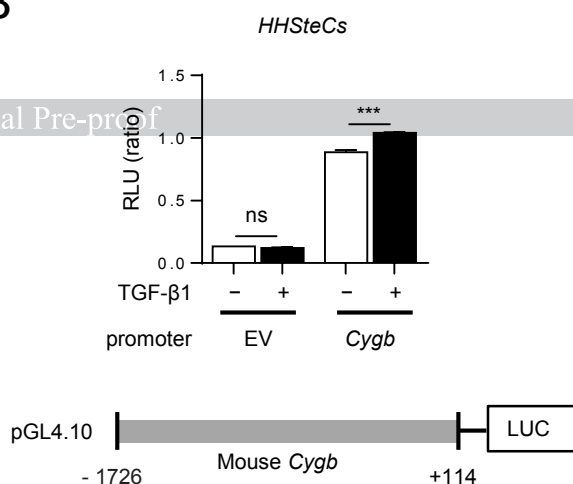


Figure 4

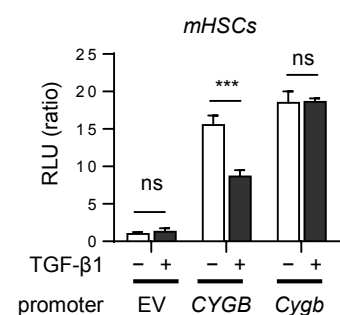
A



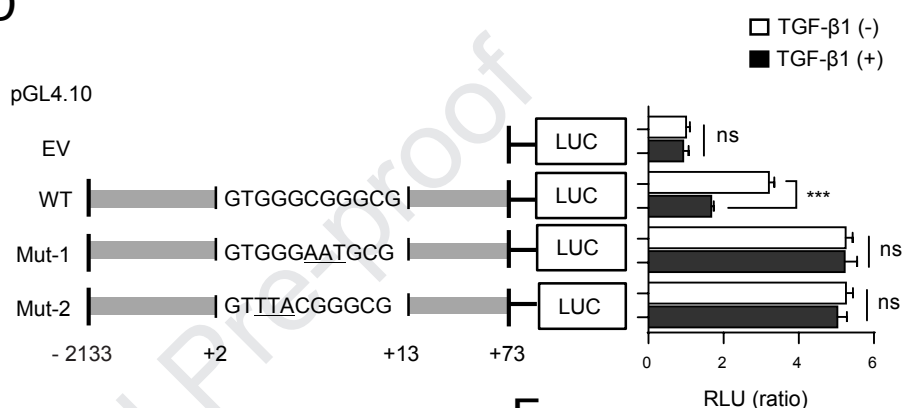
B



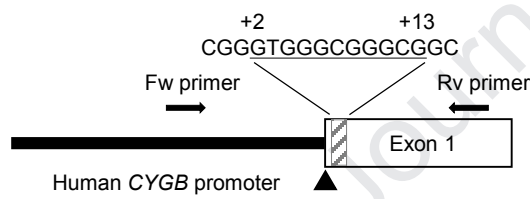
C



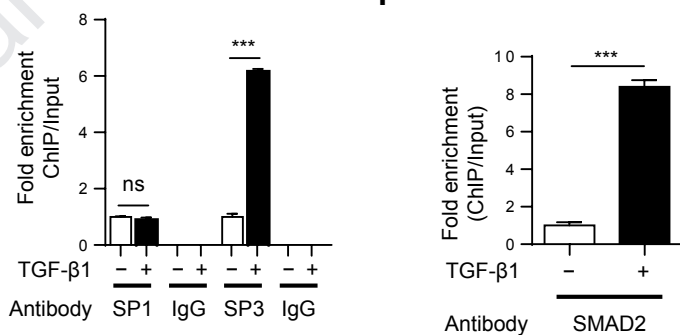
D



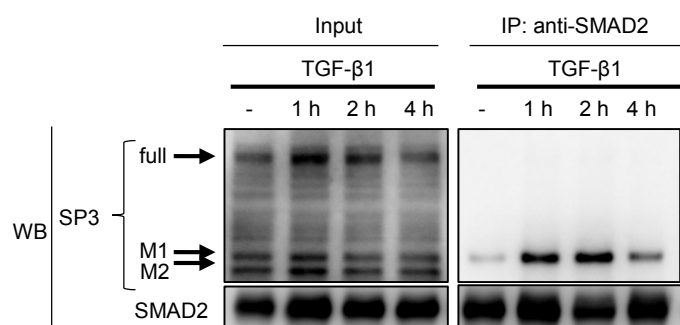
E



F



G



H

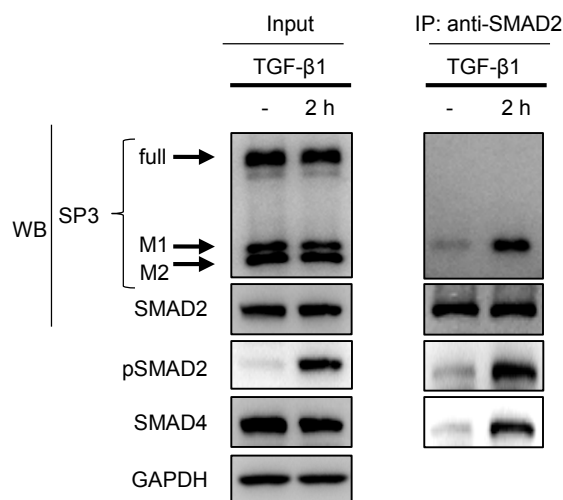
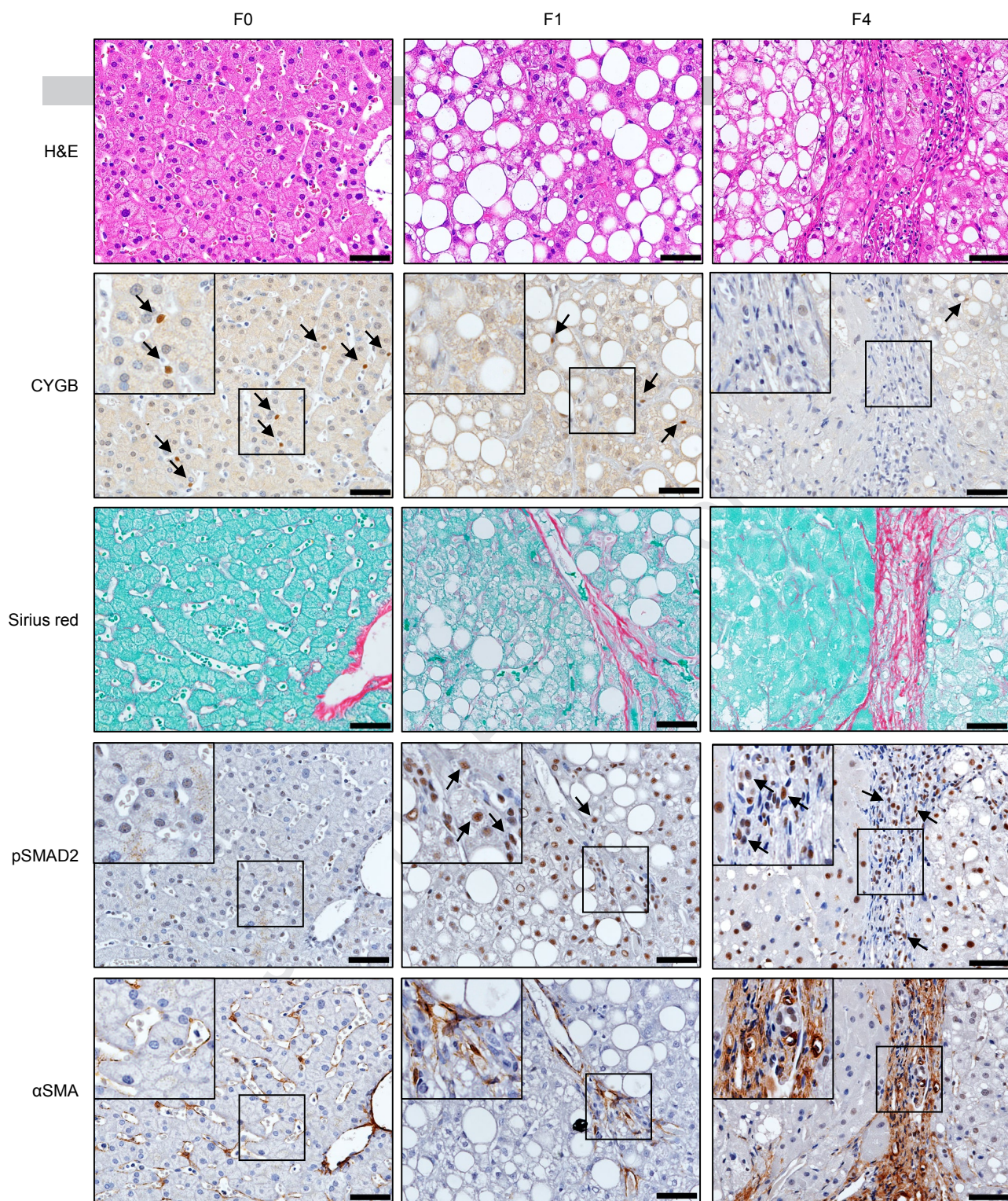
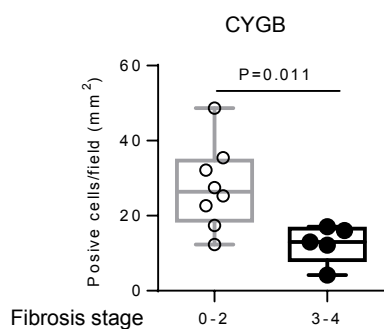


Figure 5

A



B



C

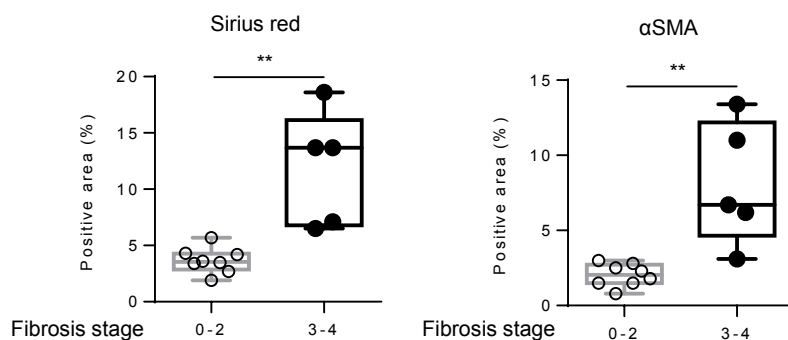
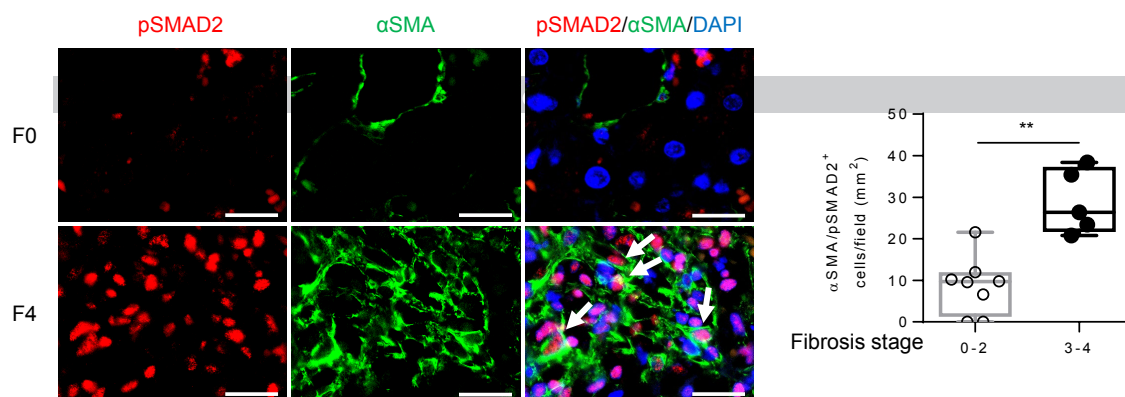
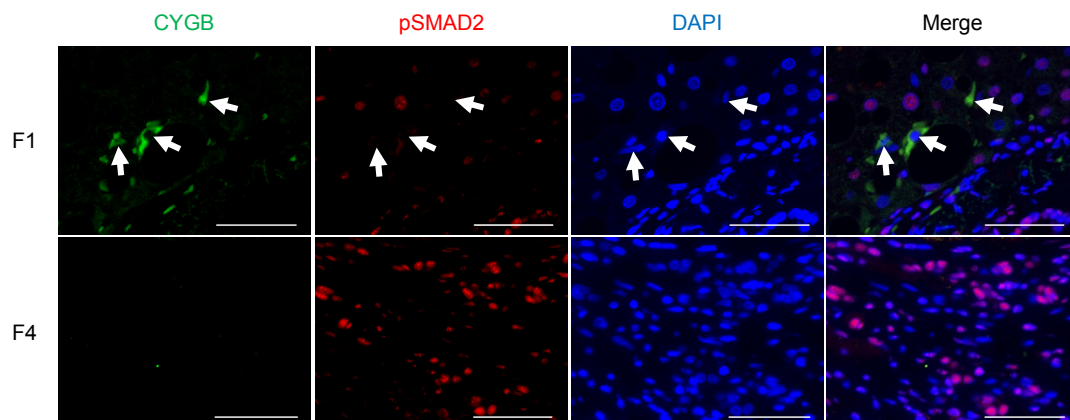


Figure 6

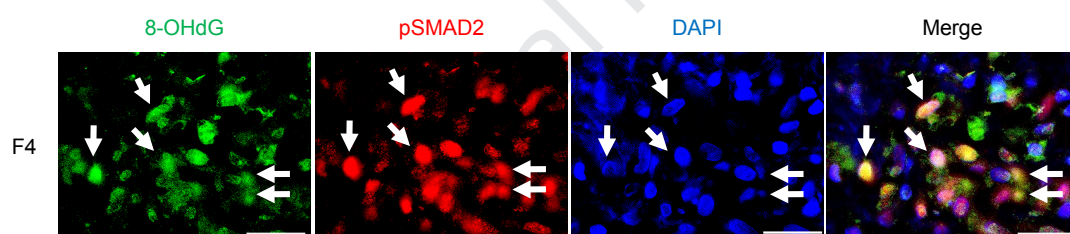
A



B



C



D

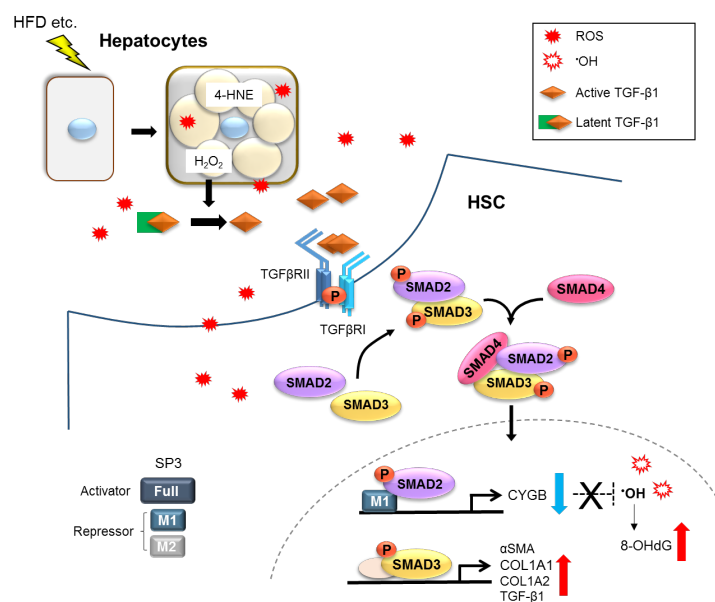


Figure 7